Turbulent Flow in Stirred Tanks

Part I: Turbulent Flow in the Turbine Impeller Region

The concept of the trailing vortex introduced by van't Riet and Smith (1975) is used for evaluation of the mean velocity and intensity of periodic velocity fluctuations in the turbine impeller discharge flow. From the analysis of forces acting on the trailing vortex, it follows that geometric similarity in the impeller discharge flow can be expected for the Reynolds number range $Re \in \langle 1.5 \times 10^4; 9.0 \times 10^4 \rangle$ and for the radial distance up to one-tenth of the impeller diameter. The calculated profiles of mean velocity and intensity of periodic velocity fluctuations agree with published data and permit the declaration of boundary conditions for the impeller discharge flow for numerical modeling of turbulent fluid flow in turbine impeller agitated tanks.

JIRI PLACEK and

L. L. TAVLARIDES

Department of Chemical Engineering
Syracuse University
Syracuse, NY 13210

SCOPE

Mixing of single and multiphase fluids in process vessels has received considerable attention in the past. There now is renewed interest due to significant energy savings to be gained and due to increasing requirements related to product quality. Detailed models of hydrodynamic flows within turbine impeller agitated tanks have been developed recently. These models require an appropriate model for the discharge flow from the turbine impeller, because this information establishes the boundary conditions and a proper accounting of the energy transmitted by the impeller to the fluid. Earlier experimental results on the discharge flow were described by phenomenological models based on the concept of the tangential jet. However, these models cannot provide information about velocity fluctuations near the impeller blades. The recent experimental results can explain the mechanism of flow within this region and the high level of velocity fluctuations. The results of these studies are employed here to construct a new model for the discharge flow from a turbine impeller based on the actual mechanism. This model will be applied in subsequent work to develop models of hydrodynamic flows within a turbine-agitated tank useful for modeling macroflow patterns, energy dissipation, micromixing of species present in the fluids and, by extension, modeling of multiphase systems.

CONCLUSIONS AND SIGNIFICANCE

The model presented of turbine impeller discharge flow is based on the geometric similarity of the trailing vortex behind the impeller blade, which was observed by van't Riet and Smith (1975); it describes the profiles of the mean velocity and the periodic velocity fluctuations near the impeller blades. The periodic contribution of kinetic energy of velocity fluctuations contains most of the energy and therefore can be used as an estimate of the overall value of energy content. The predicted dependence of turbulence dissipation rate agrees with the published data. The model is valid for turbulent flow ($Re \in \langle 1.5 \times 10^4; 9.0 \times 10^4 \rangle$) in the vicinity of the impeller ($2R/D \leq 1.3$), and for a relative size of impeller equal to or smaller than half the tank diameter. The calculated values of velocity and turbulence parameters can be used as boundary conditions for the turbine impeller discharge flow in numerical modeling of flow in agitated tanks.

INTRODUCTION

Since the pioneer work of Sachs and Rushton (1950) there have been repeated efforts to describe the fluid flow in turbine impeller agitated systems. It was found that there is an approximately linear relation between the mean impeller discharge velocity and impeller rotational speed, and that the mean velocity reaches a maximum value at the impeller disk plane. Nielsen (1958) introduced the concept of tangential jet, which permitted description of the mean

Jiří Placek is at Mokell Technical Center, CPC International Inc., Argo, IL.

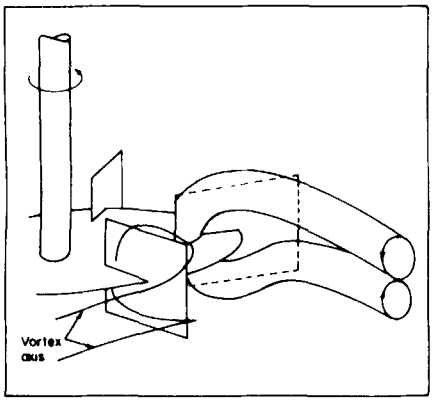

Figure 1. A pair of trailing vortexes behind the impeller blade and the positions of their axes.

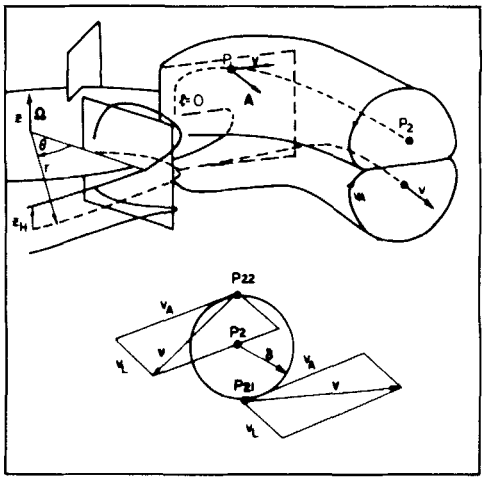

Figure 2. Coordinates in the impeller discharge flow.

velocity profiles in this region. The tangential jet model was elaborated later by DeSouza and Pike (1972) and Drbohlav et al. (1978). These models resulted in complicated correlations based on parameters with unclear physical interpretation, and they can describe only the mean velocity profiles. Cutter (1966) observed the high intensity of velocity fluctuations in the impeller discharge stream. Mujumdar et al. (1970) found that these fluctuations are of the order of the impeller tip velocity with an intensive periodic component having two peaks in the energy spectrum occurring at the value of the impeller passage frequency and at twice that value. Further, a strongly nonisotropic nature of velocity fluctuations was also recognized. The size of large energy-containing vortexes was found in these works to be about half the width of the impeller blade. However, this value is dubious as it was calculated by means of relations valid only for isotropic turbulence. This assumption of isotropic turbulence was used to compute the local turbulence dissipation rates given by Cutter (1966), Sato et al. (1970), Mujumdar et al. (1970), Komasawa et al. (1974), Nagata et al. (1975), and by others. These rates can be corrected for nonisotropic turbulence to yield reasonable energy dissipation data as it was shown by Okamoto et al. (1981) when the correction proposed by Lumley (1965) is used.

The concept of the trailing vortex was introduced by van't Riet and Smith (1975), who also quantitatively described the velocity field within it. They found that the vortex rotational velocity is of the order of impeller tip velocity and that the vortex rotation generates high velocity fluctuations in radial, axial, and tangential directions. Vortex rotation within the impeller zone was also mentioned by Günkel and Weber (1975).

VORTEX FLOW IN THE IMPELLER DISCHARGE STREAM

Van't Riet and Smith (1975) observed that the trailing vortexes originate behind the inner vertical edges of the impeller blade, one on each side of the impeller disk plane. As shown in Figure 1, the vortex flow is initially vertical toward the horizontal blade edge, where the flow direction becomes horizontal with rapid radial outflow. Before reaching the outer blade edge, both vortexes turn in a tangential direction opposite to the direction of the impeller rotation, and finally leave the impeller region in the direction approximately normal to the blade edge. At the same time the axes of both vortexes shift toward the impeller disk plane. Van't Riet (1975) found that the values of the vortex radius are greater than the distance between its axis and the impeller disk plane; therefore it can be assumed, especially near the impeller disk plane, that the shape of the vortex is deformed as shown in Figure 2. The changes of the position of the trailing vortexes result from the action of Coriolis acceleration and the velocity induced by the vortex rotation.

The Coriolis acceleration $\tilde{A}$,

$$\tilde{A} = -2\tilde{\Omega} \times \tilde{v}_{REL} \tag{1}$$

changes the vortex flow direction in the horizontal plane. Here Ω is the angular velocity of the impeller and v_{REL} is the relative velocity of the fluid with respect to the rotating coordinates. In the first phase of the vortex propagation (point P1 in Figure 2), its flow direction is almost radial and the resulting Coriolis acceleration turns the vortex strongly in the tangential direction. When the vortex direction is changed, however,the acceleration turns the vortex back toward the impeller axis. This vortex motion can be shown by comparison of the velocity components in the trailing vortex behind the impeller blade. For instance, the diametrically opposed points P21 and P22 lie on the circle with radius δ in a plane normal to the vortex axis, and the corresponding axial point P2 is a distance ℓ from the vortex origin (measured along the vortex axis). Following van't Riet and Smith, the velocities at points P21 and P22 are decomposed into a rotational velocity component v_A and a longitudinal velocity component in the direction of the vortex

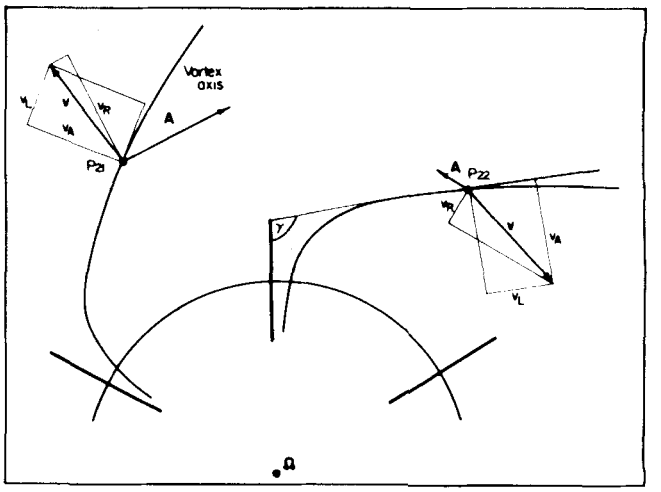

Figure 3. Action of Coriolis acceleration.

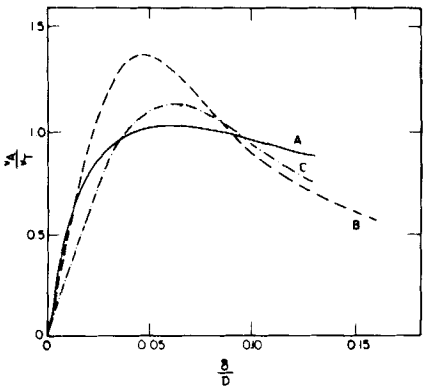

Figure 4. Dimensionless profiles of the vortex rotational velocity.

A: Data of van't Riet and Smith (1975), $Re \in \langle 1.5 \times 10^4; 9.0 \times 10^4 \rangle$.
B: Calculated from Eq. 5 with $C_1 = 0.568$ and $C_1 = 0.651$.
C: Best possible fit of Eq. 5 to the data with $C_1 = 0.613$ and $C_2 = 0.386$.

axis v_L. Also, the position of P21 on the disk plane and P22 on the top of the vortex specifies a zero velocity for the axial component v_Z. As the value of the angle γ between the blade surface and the vortex axis (Figure 3) is about 100°, and the absolute values of v_A and v_L are about the same order, the horizontal projections shown in the figure can be obtained. It is evident that the Coriolis force changes its direction, but the overall effect causes inward direction and a corresponding change in flow direction. The maximum vortex size is limited both by the size of the impeller blade and by the influence of the Coriolis force, which magnitude can be compared with the inertia forces by the Rossby number,

$$Ro = \frac{v_A}{\Lambda\Omega}. \tag{2}$$

Here v_A is the representative vortex velocity with respect to the coordinates rotating with the angular velocity Ω, and Λ is the distance over which v_A varies significantly. The greater the value of the Rossby number, the less the flow field is influenced by the Coriolis force.

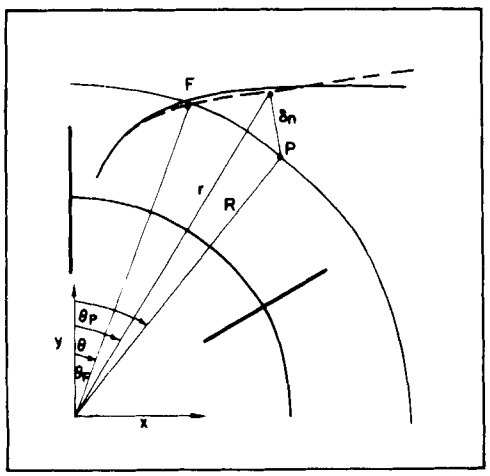

Figure 5. Coordinates in a horizontal plane and comparison of horizontal projection of the axis of the trailing vortex. ——— van't Riet and Smith (1975) for $Re \in \langle 1.5 \times 10^4; 9.0 \times 10^4 \rangle$; (- - - - - - -) Eq. 7.

The shift of trailing vortexes toward the impeller disk plane is induced by their rotation, and the velocity belonging to this displacement follows from Biot-Savart's law,

$$\tilde{v} = \frac{\Gamma}{4\pi} \int_{(L)} \frac{d\tilde{r} \times \tilde{r}}{r^3}. \tag{3}$$

Here Γ is the vortex circulation given as the integral of the vortex vorticity over the cross section area, L is the length of the trailing vortex, and $\tilde{r}$ is the radius vector of the points for which the induced velocity is evaluated. The signs of vorticities for a pair of trailing vortexes are opposite, due to their opposite directions of rotation; hence the signs of their circulations are also opposite. From Eq. 3 if follows that both trailing vortexes move toward the impeller disk plane.

Van't Riet and Smith (1975) found that the vortex rotational velocity v_A is linear in the impeller tip velocity v_T. As both the Coriolis force and the induced velocity are also linear in velocity, it can be assumed that the vortex behind the impeller blade can be normalized by the impeller diameter D and the impeller tip velocity v_T and that this model could be used for the scale-up.

VELOCITIES IN THE IMPELLER DISCHARGE STREAM

The components of vortex velocity can be calculated from the results of van't Riet and Smith (1975) if the cylindrical coordinates (r,θ,z) rotating with the impeller are used (Figure 2). From their data it follows that the longitudinal velocity along the vortex axis v_L is linear with the impeller tip velocity v_T and the dimensionless vortex coordinate ℓ/D,

$$v_L = 1.386 v_T \frac{\ell}{D}, \quad \frac{\ell}{D} \in \langle 0.3; 0.9 \rangle. \tag{4}$$

Van't Riet and Smith recommended the following equation for calculation of the vortex rotational velocity v_A,.

$$v_A = \frac{C_1}{2\pi} \frac{v_T D}{\delta} \left\{ 1 - \exp\left[-\frac{C_2}{2} \left(\frac{\delta}{D} \right)^2 \frac{v_T D}{\nu_{\text{eff}}} \right] \right\}, \tag{5}$$

where C_1 and C_2 are universal constants. They also suggested that the effective kinematic viscosity ν_{eff} can be related to the impeller tip velocity v_T. The following correlation results from their data (SI units):

$$\nu_{\text{eff}} = 0.00013 v_T, \quad Re \in \langle 1.5 \times 10^4; 9.0 \times 10^4 \rangle \tag{6}$$

with $C_1 = 0.568$ and $C_2 = 0.651$. There are discrepancies between the values determined experimentally and those calculated from Eq. 5, as is seen in Figure 4. Also, a nonlinear regression does not yield a reasonable fit of Eq. 5 to the data. In our calculations, therefore, the values of v_A interpolated from the experimental data are used.

To evaluate radial, tangential, and axial velocity components it is necessary to describe the vortex axis position in coordinates (r,θ,z). From the results mentioned above it follows that for the turbulent flow regime ($Re \in \langle 1.5 \times 10^4; 9.0 \times 10^4 \rangle$), the vortex axis maintains a constant angle γ relative to the impeller blade, and that at distances greater than $2R/D \cong 1.2$ from the vortex origin, the position of the vortex axis projected into a horizontal plane can be approximated by a straight line. From this assumption and from the data obtained in the baffled tank with diameter $T = 0.44$ m and the impeller diameter $D = 0.4T$, the following equations can be derived for the radial coordinate of the vortex axis:

$$r = |0.894\,(\theta - 0.0873)^{0.372} + 0.584|D, \quad \theta \in \langle 0.09; 0.39 \rangle,$$
$$r = \frac{D}{\cos\theta - 0.158 \sin\theta}, \quad \theta \in \langle 0.39; 0.75 \rangle. \tag{7}$$

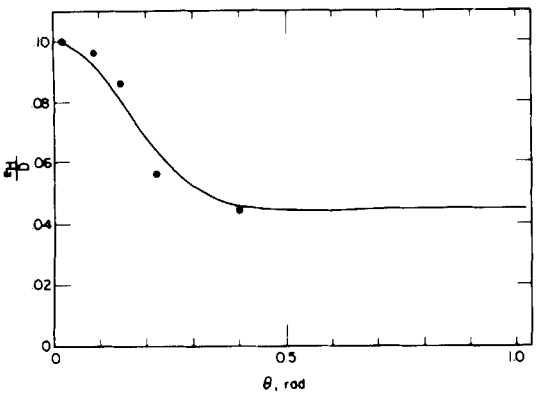

Figure 6. Comparison of vertical position of axis of trailing vortex calculated from Eq. 8 with data of van't Riet (1975) for $Re = 3.0 \times 10^5$

The predicted and experimentally observed position of vortex axis projected into a horizontal plane are compared in Figure 5. There is also a change of the axial coordinate of the vortex axis z_H. Figure 6 shows that at the beginning of the radial outflow, the vortex axis is separated from the impeller disk plane by a distance approximately equal to half the blade width. Later, when the vortex leaves the impeller zone there is a significant drop of the vortex axis position. The new axis position lies at a distance from the disk plane equal to approximately one-quarter of the width of the impeller blade. From the vortex pressure profiles published by van't Riet (1975) the correlation can be derived:

$$z_H = |0.056 \exp(-21.5\theta^2) + 0.044|D, \quad \theta \in \langle 0; 1.05\rangle. \quad (8)$$

These equations enable one to calculate the distance δ between the vortex axis and the arbitrary point P having the coordinates (R,θ_P,z). As the vortex rotates in the plane normal to its axis, this distance projected in the horizontal plane is equal to

$$\delta_H = \sqrt{(R\sin\theta_P - r\sin\theta)^2 + (R\cos\theta_P - r\cos\theta)^2}. \quad (9)$$

Here θ is the solution of the equation describing the normal of the vortex axis on which the point P lies:

$$(R\sin\theta_P - r\sin\theta)\left(r\cos\theta + \sin\theta\frac{dr}{d\theta}\right) + (R\cos\theta_P - r\cos\theta)\left(\cos\theta\frac{dr}{d\theta} - r\sin\theta\right) = 0, \quad (10)$$

and can be found numerically. The space distance of P from the vortex axis δ is

$$\delta = \sqrt{\delta_H^2 + (z - z_H)^2}. \quad (11)$$

The relation between the vortex axis coordinate ℓ and the angle θ follows from the data of van't Riet and Smith

$$\ell = (0.754\theta + 0.175)D, \quad \theta \in \langle 0.1; 0.7\rangle. \quad (12)$$

Van't Riet et al. (1976) found that the velocity component along the vortex axis v_L is constant within the trailing vortex. v_L was also assumed constant even outside the vortex as a result of uniform discharge flow from the rotating impeller zone, which is of course superposed with the vortex rotating behind the blade. Although the assumption is speculative, their velocity oscillographs seem to confirm the uniform discharge flow model. Günkel and Weber (1975) also found nearly a uniform value of radial velocity between the blades after the vortex passage. This assumption implies that the representative value of the longitudinal velocity component along the vortex axis follows from Eqs. 4 and 12

$$v_L = v_T(1.045\theta_F + 0.243), \quad \theta_F \in \langle 0.16; 0.70\rangle. \quad (13)$$

The value of θ_F is defined as the angle given by the intercept of the vortex axis and the radial distance R for which the velocity is evaluated. θ_F can be obtained as a solution of Eq. 7 for $r = R$.

The velocity components in the nonrotating Cartesian base located at the intercept of the impeller axis and the horizontal impeller symmetry plane can be then written as

$$v_X = v_L\cos(\tan^{-1}K_F + \theta_F - \theta_P) - v_T\frac{R}{r}\cos\theta_P + v_A\frac{z - z_H}{\delta}\cos\left(\tan^{-1}\frac{1}{K}\right), \quad (14)$$

$$v_Y = v_L\sin(\tan^{-1}K_F + \theta_F - \theta_P) + v_T\frac{R}{r}\sin\theta_P - v_A\frac{z - z_H}{\delta}\sin\left(\tan^{-1}\frac{1}{K}\right), \quad (15)$$

$$v_Z = v_A\frac{R - r}{\delta}, \quad (16)$$

where K is the tangent of the vortex axis,

$$K = \frac{d(r\cos\theta)}{d\theta}\frac{d\theta}{d(r\sin\theta)}. \quad (17)$$

A similar equation can be written for K_F with $\theta = \theta_F$,

$$K_F = \left[\frac{d(r\cos\theta)}{d\theta}\frac{d\theta}{d(r\sin\theta)}\right]_{\theta=\theta_F}. \quad (18)$$

Equations 14–18 describe the velocity within the impeller stream as a result of the interaction of the uniform impeller discharge flow and the trailing vortex behind the impeller blade. There are, however, two vortexes behind each blade (the other one located at the opposite horizontal blade edge). It could be assumed, especially near the impeller disk plane, that the resultant velocity will depend on both vortexes. This assumption would be true in this work if the data of van't Riet and Smith (1975) in Figure 4 were based on velocity measurements within a single vortex. However, as van't Riet and Smith measured vortex rotational velocity v_A in a system where one vortex had to be influenced by the opposite one, it can be deduced that their data describe the combined effect of both vortexes.

The x-y velocity components can be transformed in cylindrical velocity components with respect to the nonrotating base,

$$v_R = v_X\sin\theta_P + v_Y\cos\theta_P, \quad (19)$$

$$v_\theta = v_X\cos\theta_P - v_Y\sin\theta_P. \quad (20)$$

The value of mean velocity components for the six-bladed turbine impeller is obtained by integration over a 60° interval,

$$\bar{v}_i = \frac{3}{\pi}\int_0^{\pi/3} v_i d\theta_P, \quad i = R,\theta,Z \quad (21)$$

and the value of mean velocity $\bar{v}$ is then

$$\bar{v} = \sqrt{\bar{v}_R^2 + \bar{v}_\theta^2 + \bar{v}_Z^2}$$

The known values of the mean velocity components permit the evaluation of the intensity of the periodic velocity fluctuations from

$$\overline{v_i'^2} = \frac{3}{\pi}\int_0^{\pi/3}(v_i - \bar{v}_i)^2 d\theta_P, \quad i = R,\theta,Z \quad (23)$$

DISCUSSION

Velocity profiles and turbulence parameters calculated by means of the preceding equations are compared here with the available experimental data published by others. These data can be divided

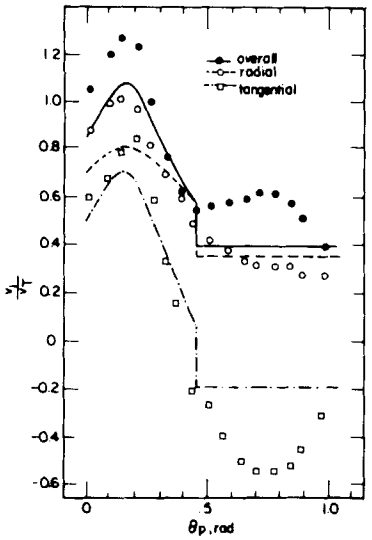

Figure 7. Comparison of calculated values of velocity and its components relative to the coordinates rotating with the impeller, with the data of Günkel and Weber (1975): air is the working fluid; D = 0.228 m; $Re = 3.8 \times 10^4$; position in impeller disk plane at distance $R/D = 0.912$.

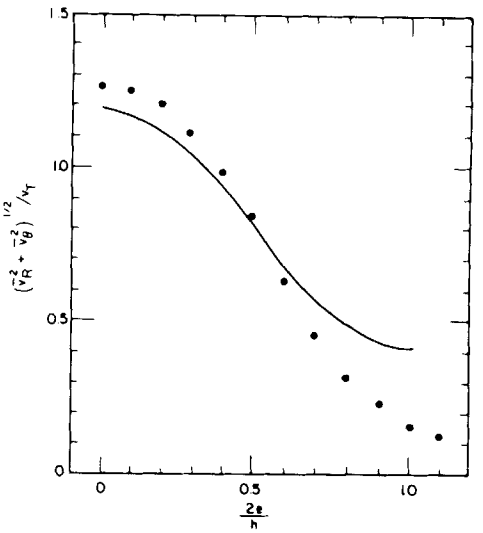

Figure 8. Comparison of calculated axial profile of mean velocity in a horizontal plane with the data of Günkel and Weber (1975), measured in air with D = 0.228m, $Re = 3.8 \times 10^4$ in radial distance $2R/D$ = 1.09.

into three groups: velocity profiles measured by a probe which rotates with the impeller, mean velocity profiles measured by a fixed probe, and intensity of velocity fluctuations.

The only velocity profile measured by the probe rotating with the impeller is that published by Günkel and Weber (1975). They used a shielded hot wire probe positioned 10 mm inward from the blade tip in the impeller disk plane The velocity profile measured between the impeller blades is shown in Figure 7. These experimental values are compared with the velocity predicted by the present model by employing transformation into the coordinates rotating with the impeller. The values of velocity components predicted by this model are about 18% lower than those observed experimentally. This difference is probably caused by the use of the average vortex rotational velocity (Figure 4), since the actual rotational velocity is somewhat larger in the impeller disk plane due to interaction with the other vortex and the asymmetry of these vortexes. The drop of the tangential velocity component for higher values of θ_P is explained by the presence of another vortex with opposite direction of rotation which is located between the mean trailing vortex and the following blade. There is no other evidence of the presence of this vortex between the impeller blades, and this vortex was not observed by van't Riet outside the rotating impeller zone. Even if this secondary vortex exists, it can be expected that it is more intensively destroyed by the action of Coriolis force than is the main vortex. The size of the secondary vortex can be taken from Figure 7 as 1.8× the size of the main vortex, and its rotational speed is approximately 0.6× the rotational velocity of the main vortex. From Eq. 3 it follows that the ratio of Rossby numbers of the main to the secondary vortex is about 3, and the secondary vortex is therefore assumed to be three times more rapidly destroyed within the impeller discharge flow.

Günkel and Weber (1975) also published axial profiles of the mean velocity measured in the same system 10 mm from the impeller blade tip. From Figure 8 it is seen that the values of predicted and experimentally determined mean velocity in the horizontal plane are in good agreement near the impeller symmetry plane. However, differences up to 20% (relative to the velocity in the impeller disk plane) occur near the edge of the blade. This discrepancy may be due to the asymmetry of the trailing vortex, and due to the assumption of axially uniform outflow from the impeller zone as it was used in derivation of Eq. 13. The axial component of the mean velocity in the impeller disk plane calculated from Eq. 21 is not equal to zero as a result of the approximation of the asymmetric trailing vortex by a circular cylinder. This false mean axial velocity component is 7% of the mean overall velocity.

The values of relative intensity of velocity fluctuations generated by the trailing vortex passage predicted by this model are compared with those published by Günkel and Weber (1975) in Figure 9. The shielded hot wire probe was oriented in the mean velocity direction, and the measured RMS value of velocity fluctuation was normalized by the mean velocity in the impeller disk plane. In Figure 9 periodic fluctuation data are plotted. The values calculated from Eq. 23 were projected into the direction of the mean horizontal velocity by means of the transformation

$$\sqrt{\overline{v_{HOR}^2}} = \frac{\sqrt{\overline{v_R^2}}\,\bar{v}_\theta + \sqrt{\overline{v_\theta^2}}\,\bar{v}_R}{(\sqrt{\bar{v}_R^2 + \bar{v}_\theta^2})_{z=0}} \cdot \qquad (24)$$

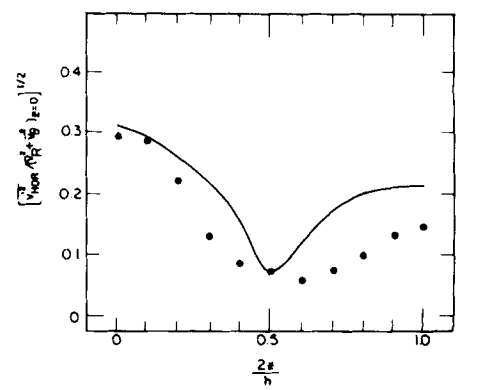

Figure 9. Comparison of calculated axial profile of relative intensity of periodic velocity fluctuations in a horizontal plane with the data of Günkel and Weber (1975): air is the working fluid; D = 0.228 m; $Re = 6.0 \times 10^4$; position at radial distance $2R/D$ = 1.09.

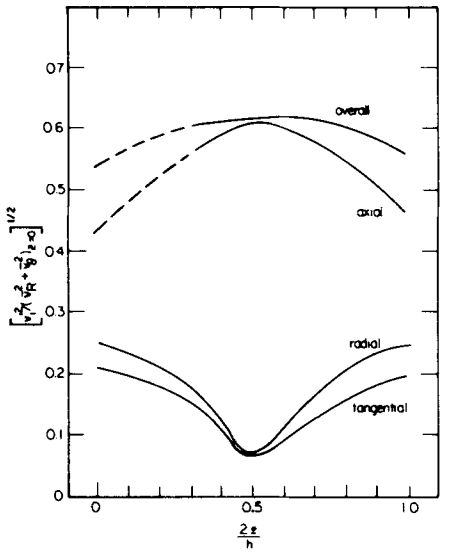

Figure 10. Calculated axial profiles of overall relative intensity of periodic velocity fluctuations and its components in radial distance $2R/D = 1.09$.

Good agreement is obtained in the impeller symmetry plane but differences occur with increasing distance from the impeller disk plane (where the calculated values of relative intensity of velocity fluctuations are higher). The difference observed with increasing distance can be explained with similar assumptions as in the case of the mean velocity profile. The trailing vortex also generates intensive periodic fluctuations in the vertical direction with maximum values at distances halfway between the blade edge and the impeller disk plane. Relative intensities reach values over 60% (with respect to the mean velocity in the impeller disk plane). The high intensity of vertical velocity fluctuations was observed by Drbohlav et al. (1978) and Fořt et al. (1979).

The model presented cannot be used to predict the mean velocity decay with increasing distance from the impeller, as the trailing vortex exists only up to a limited distance from the impeller. The model is also severely limited by the assumption that the trailing vortexes are carried by the uniform outflow from the impeller zone which can be applied only in the vicinity of the impeller. The geometric similarity of the trailing vortexes behind the turbine impeller blade in turbulent flow observed by van't Riet and Smith (1975) on which Eqs. 14–18 are based is confirmed by data of Mujumdar et al. (1970) and Günkel and Weber (1975). These investigators obtained observations in different apparatus and employed different working fluids. The measurements of van't Riet and Smith employed the relative impeller diameter $D/T = 0.4$ while Mujumdar et al. used a smaller impeller ($D/T = 0.33$) and Günkel and Weber a larger one ($D/T = 0.5$). They all found that for varying impeller rotational speeds the periodic velocity fluctuations disappeared at the same relative distance from the impeller, approximately $2R/D = 1.4$. It should be mentioned that Nagata et al. (1975) observed a significant increase of the dissipation rate of turbulence at the same distance. These observations support the model based on the dominating effect of Coriolis force on the trailing vortex, and they also indicate that the distance from the tank wall does not significantly influence the decay of the trailing vortex for the impeller diameters $D/T \in \langle 0.33; 0.5 \rangle$.

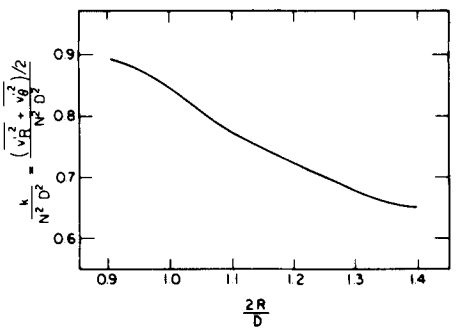

Figure 11. Calculated radial profile of kinetic energy of velocity fluctuations in impeller disk plane.

MODELING THE VELOCITY FLUCTUATIONS

It is seen in the energy spectra published by Mujumdar et al. (1970), Günkel and Weber (1975), van't Riet et al. (1976), that most of the energy of the velocity fluctuations is contained in the trailing vortexes. The overall kinetic energy can be therefore approximated by means of Eq. 23 as

$$k = \frac{1}{2}(\overline{v_R'^2} + \overline{v_\theta'^2} + \overline{v_Z'^2}) = \frac{1.5}{\pi}\int_0^{\pi/3} (v_R - \bar{v}_R)^2 + (v_\theta - \bar{v}_\theta)^2 + (v_z - \bar{v}_z)^2 |d\theta_P \quad (25)$$

The intensity of the velocity fluctuations in the axial direction near the impeller disk plane calculated from Eq. 23 is not equal to zero as a result of the approximation of the asymmetric trailing vortex by a circular cylinder. Accordingly, calculations of k for the symmetry axis should be made with the value of $\overline{v_Z'^2}$ set to zero to better approximate the actual value of the kinetic energy. From Figure 10 it follows, however, that the calculated sum of intensities of velocity fluctuations remains almost constant between the impeller disk plane and the blade edge.

The value of k calculated from Eq. 25 slightly decreases with the radial distance from the impeller, Figure 11. This slow decrease corresponds with the data of Mujumdar et al. and Günkel and Weber who did not find significant changes or relative intensity of velocity fluctuations within the range $2R/D \in \langle 1.0; 1.3 \rangle$ where the mean velocity was also almost constant. From these results it is seen that the calculated profiles of the kinetic energy of the periodic velocity fluctuations do not change significantly in either axial or radial directions, and that the value of k in the vicinity of the impeller blades can be assumed constant and proportional to the squared impeller tip velocity.

This model cannot be directly used to predict the value of the dissipation rate of turbulence ϵ. Some assumptions concerning the dissipation rate arise, however, when a relation of dimensional validity

$$\epsilon \sim \frac{k^{3/2}}{\Lambda} \quad (26)$$

is used. This equation is derived by use of the assumption of a constant energy transfer rate through the entire cascade of vortexes, from large energy-containing ones to the smallest dissipation eddies. Due to the periodicity and the complicated nature of the fluid flow in the impeller region, the values of macroscales published by Cutter (1966), Mujumdar et al. (1970), and Komasawa et al. (1974) display great variance. Further, the values of Λ published by Cutter and Mujumdar et al. differ significantly in radial and axial directions, in spite of the approximately cylindrical cross section of the trailing vortexes. The trailing vortexes are stable and their size follows from the data of van't Riet and Smith (1975).

In order to apply Eq. 26 it is necessary to determine the mag-

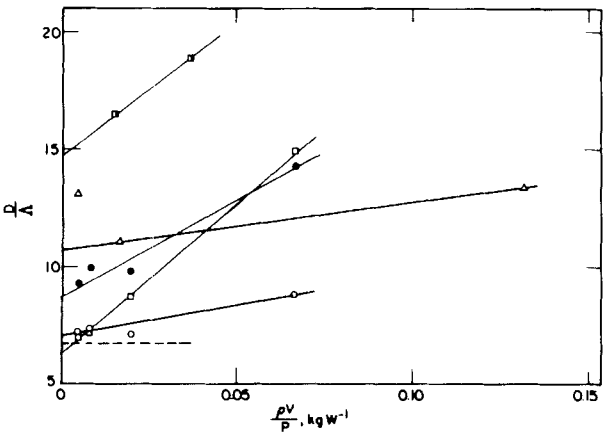

Figure 12. Values of dimensionless macroscale of velocity fluctuations extrapolated from the data of Günkel and Weber (1975) and their comparison with the prediction from Eq. 27 (broken lines). For symbols see Table 1.

nitude of the length scale Λ. Since the righthand side of this equation describes the rate of energy transfer from large vortexes, the value of Λ must be of order of their size, i.e., close to the macroscale of velocity fluctuations. It is evident that the macroscale of velocity fluctuations is related to the diameter of the trailing vortex. From Figure 4 it follows that the vortex rotational velocity reaches a maximum at about $\delta = 0.06D$ and the value of Λ is therefore about $0.12D$. Another representative size of the trailing vortex can be taken as an average weighted by the kinetic energy belonging to the given distance from the vortex axis,

$$\frac{\Lambda}{D} = 2\,\frac{\int_0^{0.13} \delta/D\, v_A^2\, d(\delta/D)}{\int_0^{0.13} v_A^2\, d(\delta/D)}. \tag{27}$$

The value of Λ calculated from this equation using the data of van't Riet and Smith (1975) is slightly higher, $\Lambda = 0.146D$. Cutter (1966), Mujumdar et al. (1970) and Komasawa et al. (1974) found approximately half this value ($\Lambda/D \in \langle 0.03; 0.1 \rangle$). Komasawa et al. interpret the data of Cutter and Mujumdar et al. as showing a moderate dependence of Λ on distance from the impeller. Over a limited range of radial distances ($2R/D \in \langle 1.1; 1.6 \rangle$), however, considerable scatter in the complete set of experimental data exists so that no noted dependency of Λ on the distance from the impeller applies here. Also, the results for Λ were obtained by means of relations valid only for isotropic turbulence. Values of the macroscale of turbulence approximately equal to the half-blade width were found by Günkel and Weber (1975) in the bulk of agitated tanks outside the impeller stream, where the turbulence can be regarded as isotropic. It can be assumed that in spite of the lost vortex orientation due to the action of Coriolis force, the original size of the vortex can be detected at even greater distances from the impeller, as the rate of energy transfer through the cascade of vortexes is not infinite. The original size of large vortexes can be then estimated from the assumption that with increasing power input the original size of vortexes is more conserved within the tank volume. The impeller power input per unit mass can be expressed from the correlation of Schwartzberg and Treybal (1968) as

$$\frac{P}{\rho V} = 7.9\,\frac{N^3D^5}{T^2H}, \tag{28}$$

Table 1. Data Plotted in Figure 12: Macroscale of Velocity Fluctuations in Impeller Discharge Flow

D,m	h/D	T/D	$Re \times 10^4$	z/D	Λ/D	Symbol	
0.305	0.2	3.0	6.8-9.0	−0.025	0.068	■	Data of Günkel and Weber (1975) extrapolated from Figure 12.
0.228	0.4	2.0	2.5-6.0	−0.16	0.114	●	
0.228	0.4	2.0	2.5-6.0	−0.33	0.139	○	
0.228	0.2	2.0	2.5-6.0	−0.26	0.156	□	
0.457	0.2	2.0	5.0-15.0	0.25	0.083	△	
			1.5-9.0		0.146	Eq. 27	

and the original vortex size follows from the limit

$$\frac{D}{\Lambda} = \lim_{N \to \infty} F\left(\frac{T^2H}{7.9N^3D^5}\right). \tag{29}$$

The results are shown in Figure 12, for the data listed in Table 1. As the rotational velocity of the trailing vortex is equal approximately to the impeller tip velocity, the value D/Λ is also equal to the Rossby number. In spite of the variance of the data it can be assumed that the original size of the large vortexes is greater than $0.1D$ for a tank with diameter $T = 0.228$ m, and this value does not change significantly with doubled blade width. The values of Λ/D detected in a large tank with diameter $T = 0.457$ m are smaller. This can be caused by the greater inhomogeneity in a larger tank, as Günkel and Weber (1975) presented average radial profiles for the constant axial coordinate. This analysis shows that a reasonable value of Λ is approximately $0.14D$.

A rough estimate of the dissipation rate of turbulence can now be made using the $\Lambda = 0.14D$ value, Figure 11, and Eq. 26 to obtain:

$$\epsilon = \frac{(0.8N^2D^2)^{3/2}}{0.14D} = 5.1N^3D^2. \tag{30}$$

As Eq. 28 also expresses the volume mean value of dissipation rate $\bar{\epsilon}$, the ratio $\epsilon/\bar{\epsilon}$ should be independent of impeller rotational speed N if the tank geometry is unchanged:

$$\epsilon/\bar{\epsilon} \sim \frac{T^2H}{D^3} \tag{31}$$

This is confirmed by the results of Okamoto et al. (1981), who did not find differences in local values of $\epsilon/\bar{\epsilon}$ in the interval $Re \in \langle 8.0 \times 10^3; 1.2 \times 10^5 \rangle$ using tanks with diameters $T = 0.15$ m, $T = 0.3$ m, and $T = 0.6$ m, height $H = T$, impeller of diameter $D = 0.5T$, and water as a working fluid. The values of ϵ were calculated from one-dimensional energy spectra where local isotropy of turbulence was assumed, and the calculated results were corrected for the shear flow by the correction proposed by Lumley (1965). In spite of the introduced simplifications, their data seem to be reasonable, as the integral of local dissipation rates over the entire tank volume agrees with the impeller power input calculated from power correlation. They found the average values $\epsilon/\bar{\epsilon} = 5.9$ for the distance $2R/D = 1.14$ and $\epsilon/\bar{\epsilon} = 5.2$ for $2R/D = 1.4$, respectively. The value of $\epsilon/\bar{\epsilon}$ calculated from Eqs. 28 and 30 is

$$\epsilon/\bar{\epsilon} = \frac{5.1N^3D^2}{7.9\,\dfrac{N^3D^5}{(2D)^3}} = 5.16 \tag{32}$$

which is in good agreement with the preceding data.

It is therefore suggested that Eqs. 25 and 30 provide reasonable assumptions of turbulence parameters in the turbine impeller discharge flow.

ACKNOWLEDGMENT

The financial support provided by National Science Foundation Grant CPE-80-21039 is gratefully acknowledged. Constructive comments by Mr. G. W. Smith are appreciated.

NOTATION

A = Coriolis acceleration
C_1 = constant, Eq. 5
C_2 = constant, Eq. 5
D = impeller diameter
H = tank height
K, K_F = tangents of vortex axis
k = kinetic energy of velocity fluctuations
L = distance
ℓ = distance measured along vortex axis
N = impeller rotational speed
P = impeller power input
R = radial coordinate, Figure 5
Re = Reynolds mixing number, ND^2/ν
Ro = Rossby number, Eq. 2
r = radial coordinate of vortex axis
$\tilde{r}$ = radius vector
T = tank diameter
V = tank volume
$\bar{v}$ = mean velocity
$\tilde{v}$ = velocity vector
v' = fluctuating velocity
v_A = circumferential velocity within trailing vortex
v_L = velocity component along trailing vortex axis relative to rotating impeller
v_{HOR} = fluctuating velocity projected into impeller disk plane
v_R = radial velocity component
v_{REL} = relative velocity with respect to rotating coordinates
v_T = impeller tip velocity
v_X, v_Y, v_Z = Cartesian components of velocity
v_θ = tangential velocity component
z = axial coordinate
z_H = axial coordinate of trailing vortex axis

Greek Letters

γ = angle between blade surface and vortex axis, Figure 3
Γ = circulation of trailing vortex
δ = distance from axis of trailing vortex, Figure 2
δ_H = horizontal projection of δ
θ = tangential coordinate of trailing vortex axis
θ_P = angle, Figure 5
θ_F = angle, Figure 5
Λ = macroscale of velocity fluctuations
ν_{eff} = effective kinematic viscosity
ρ = density
Ω = impeller angular velocity
ϵ = local dissipation rate of turbulence
$\bar{\epsilon}$ = tank volume average value of ϵ

LITERATURE CITED

Cutter, L. A., "Flow and Turbulence in a Stirred Tank," *AIChE J.*, **12**, 35 (1966).

DeSouza, A., and R. W. Pike, "Fluid Dynamics and Flow Patterns in Stirred Tanks with a Turbine Impeller," *Can. J. Chem. Eng.*, **50**, 15 (1972).

Drbohlav, J., et al., "Turbulent Characteristics of Discharge Flow from the Turbine Impeller," *Coll. Czech. Chem. Commun.*, **43**, 3,148 (1978).

Fořt, I., et al., "The Flow of Liquid in a Stream from the Standard Turbine Impeller," *Coll. Czech. Chem. Commun.*, **44**, 700 (1979).

Günkel, A. A., and M. E. Weber, "Flow Phenomena in Stirred Tanks," *AIChE J.*, **21**, 931 (1975).

Komasawa, I., R. Kuboi, and T. Otake, "Fluid and Particle Motion in Turbulent Dispersion. I," *Chem. Eng. Sci.*, **29**, 641 (1974).

Lumley, J. L., "Interpretation of Time Spectra Measured in High-Intensity Shear Flows," *Phys. Fluids*, **8**, 1,056 (1965).

Mujumdar, A. S., et al. "Turbulence Parameters in a Stirred Tank," *Can. J. Chem. Eng.*, **48**, 519 (1974).

Nagata, S., et al. *Mixing-Principles and Application*, 158, Halsted Press, J. Wiley & Sons, New York (1975).

Nielsen, H. J., "Flow and Turbulence from a Flat Blade Turbine Mixing Impeller," Ph.D. Thesis, Illinois Inst. Tech., Chicago (1958).

Okamoto, Y., M. Nishikawa, and K. Hashimoto, "Energy Dissipation Rate Distribution in Mixing Vessels and Its Effects on Liquid-Liquid Mass Transfer," *Int. Chem. Eng.*, **21**, 88 (1981).

Sachs, J. P., and J. M. Rushton, "Discharge Flow from Turbine-Type Mixing Impellers," *Chem. Eng. Prog.*, **50**, 597 (1950).

Sato, Y., M. Kamiwano, and K. Yamamoto, "Turbulent Flow in a Stirred Vessel—Effect of Impeller Types," Kagaku Kogaku, **34**, 104 (1970), in Japanese.

Schwartzberg, H. G., and R. E. Treybal, "Fluid and Particle Motion in Turbulent Stirred Tanks," *Ind. Eng. Chem. Fund.*, **7**, 1 (1968).

van't Riet, K., "Turbine Agitator Hydrodynamics and Dispersion Performance," Ph.D. Thesis, Tech. Univ. of Delft, Delft (1975).

van't Riet, K., and J. M. Smith, "The Trailing Vortex System Produced by Rushton Turbine Agitators," *Chem. Eng. Sci.*, **30**, 1,093 (1975).

van't Riet, K., W. Bruijn, and J. M. Smith, "Real and Pseudoturbulence in the Discharge Stream from a Rushton Turbine," *Chem. Eng. Sci.*, **31**, 407 (1976).

Manuscript received May 12, 1982; revision received May 2, 1983, and accepted May 19.